ORAL/POSTER REFERENCE: ICF108920R

MICROMECHANICAL MODELING OF HYDROGEN-INDUCED FRACTURE MODES IN IN903

B.P. Somerday and N. R. Moody

Sandia National Laboratories, Livermore, CA 94550, USA

ABSTRACT

Previous slow crack growth results for the austenitic Fe-Ni-Co superalloy IN903 in hydrogen gas demonstrated that the near-threshold fracture mode was a function of grain size. For grain sizes of 23 μm and 49 μm, hydrogen-induced fracture was intergranular. At larger grain sizes of 114 μm, 172 μm, and 200 μm the hydrogen-induced fracture mode changed to slip-band cracking. This transition in fracture mode from intergranular cracking to slip-band failure with increasing grain size results from competing hydrogen-induced fracture mechanisms. A stress-based micromechanical fracture model predicts that the resistance to intergranular cracking increases with increasing grain size. In addition, a strain-based model predicts that the grain size-independent slip-band fracture resistance is of the same order as the intergranular cracking resistance. The predicted fracture-resistance trends intersect at a grain size of about 100 μm, which supports the observed fracture-mode transition between grain sizes of 49 μm and 114 μm.

KEYWORDS

Hydrogen, fracture, superalloys, micromechanical modeling

INTRODUCTION

Results for the austenitic Fe-Ni-Co superalloy IN903 demonstrated that the mode of hydrogen-induced slow crack growth was sensitive to changes in both microstructure and magnitude of the applied stress-intensity factor (K). Constant-displacement experiments on wedge-opening load specimens in 207 MPa hydrogen gas at 25^{o}C showed that stage II cracking at high K levels was intergranular and independent of grain size from 23 μm to 200 μm (Figures 1(a) and 1(c)) [1, 2]. As K approached threshold (stage I) in specimens having grain sizes of 114 μm, 172 μm, and 200 μm, hydrogen-induced fracture transitioned to a mixed mode with slip-band failure predominating over intergranular cracking (Figure 1(d)). In contrast, stage I cracking in specimens having grain sizes of 23 μm and 49 μm remained intergranular (Figure 1(b)).

The transition in near-threshold fracture mode from intergranular to slip-band cracking as grain size increased (Figure 1(b) compared to Figure 1(d)) can be viewed in terms of either competing hydrogen transport paths or competing hydrogen-induced fracture mechanisms. Considering the former scenario, hydrogen is likely transported from the crack-tip surface to process-zone fracture sites through both transgranular and intergranular mechanisms. Hydrogen accumulates at transgranular sites *via* numerous lattice transport paths intersecting the crack-tip surface. While the number of transport paths is more limited along grain boundaries compared to the lattice, hydrogen may diffuse more rapidly along grain-

boundary paths [3, 4]. Assuming that hydrogen must diffuse over a distance that scales with grain size to enable grain-boundary fracture, relatively short diffusion distances in small-grain-size IN903 coupled with rapid hydrogen transport along grain boundaries may have promoted near-threshold intergranular cracking. As grain size increased, diffusion distances for grain-boundary fracture became greater and sufficient time was allowed for hydrogen accumulation at transgranular sites to promote slip-band cracking.

Hydrogen-induced fracture was intergranular in large-grain-size IN903 during stage II cracking (Figure 1(c)), which indicates that hydrogen readily diffused along grain boundaries in these microstructures. These stage II results suggest that hydrogen should be similarly supplied to grain boundaries in stage I to allow intergranular cracking in large-grain-size IN903, assuming that hydrogen-diffusion distances in stage I are comparable to those in stage II. This argument opposes the idea that competing hydrogen-transport mechanisms govern the grain size-dependent fracture-mode transition in stage I. Alternately, the transition from intergranular fracture to predominantly slip-band cracking as grain size increased (Figure 1(b) compared to Figure 1(d)) can be attributed to crack-tip mechanics and microstructure.

Micromechanical fracture models can provide insight into the roles of crack-tip mechanics and microstructure in governing hydrogen-induced fracture modes. Threshold K (K_{TH}) for intergranular slow crack growth in IN903 exposed to hydrogen gas was well-described using a stress-based micromechanical model, which proposes that fracture proceeds when the crack-tip normal stress exceeds the local fracture stress over a characteristic distance [1, 2]. This distance, related to microstructure, was associated with the grain size in IN903 [5]. In addition, slip-band cracking in hydrogen-charged IN903 during rising-displacement fracture toughness tests was accurately modeled using a strain-based micromechanical approach [1, 2, 6]. The premise of this model is similar to the stress-based model, *viz*, fracture proceeds when the crack-tip effective plastic strain exceeds the local fracture strain over a characteristic distance. For hydrogen-induced slip-band cracking in IN903, application of the strain-based model to rising-displacement fracture toughness data (K_{IH}) suggested that matrix carbide particles defined the characteristic distance [1, 2, 6].

The objective of this work is to apply stress- and strain-based micromechanical fracture models to understand the grain size-dependent transition from intergranular cracking to slip-band failure in IN903 during stage I slow crack growth in hydrogen gas. These models are analyzed using tensile data as well as rising-displacement fracture toughness and slow crack growth results from previous hydrogen-induced fracture studies of IN903.

RESULTS AND DISCUSSION

Micromechanical models are applied to near-threshold slow crack growth in IN903 to assess whether fracture-mode transitions are due to a competition between stress-based intergranular fracture and strain-based slip-band cracking. The stress-based model requires a solution for crack-tip normal stress, data for the local grain-boundary fracture stress, the characteristic microstructural fracture distance, and material deformation properties. Formulation of this model is based on elastic-plastic crack-tip stress solutions from Tracey [7] and Schwalbe [8] as described elsewhere [1, 2]. Local grain-boundary fracture stresses were estimated from hydrogen-induced tensile fracture data, which yielded values that were pertinent to the crack-tip hydrogen concentration during slow crack growth [1, 2]. These values are given in Table 1 and show that fracture stress depends on grain size. The characteristic fracture distance is assumed to equal the grain size. Deformation properties include a yield stress of 1100 MPa and strain-hardening exponent of 0.15 [1].

Model predictions of K_{TH}, assuming stress-controlled intergranular slow crack growth at all grain sizes, are shown in Figure 2. This model demonstrates that K_{TH} for stress-controlled intergranular fracture increases as grain size increases. (The trend line in Figure 2 does not include calculated K_{TH} at a grain size of 23 μm. This value equaled 37 MPa√m and was judged to be erratically high.)

TABLE 1
LOCAL FRACTURE STRESS FOR IN903 AS A FUNCTION OF GRAIN SIZE

Grain Size (μm)	Fracture Stress (MPa)
23	3007
49	2170
114	1543
172	1321
200	1251

A simple expression was derived for strain-controlled K_{TH} from crack-tip effective plastic strain, local fracture strain (ε_f^*), characteristic microstructural fracture distance (l^*), and material deformation properties (flow stress, σ_o, and elastic modulus, E), i.e., $K_{TH}=6[\sigma_o E\varepsilon_f^* l^*]^{1/2}$ [1, 2, 6, 9-11]. This model accurately described slip-band fracture in hydrogen-charged fracture toughness specimens of IN903.

To apply the strain-based model to the case of slip-band fracture during slow crack growth, estimates of ε_f^* are needed as a function of grain size and for the crack-tip hydrogen concentration that develops from exposure to 207 MPa hydrogen gas. Crack-tip fracture strains are assumed to be independent of grain size since rising-displacement fracture toughness, K_{IH}, and fracture modes for hydrogen-charged specimens were constant as a function of grain size [1, 2, 6]. Local fracture strain as a function of hydrogen concentration up to 5000 appm was estimated using void dimensions measured from hydrogen-charged fracture toughness specimens coupled with a void-growth model [2, 6]. These values are listed in Table 2. The fracture strain for slow crack growth in 207 MPa hydrogen gas is determined from extrapolating the results in Table 2 to the estimated crack-tip hydrogen concentration of 11,200 appm ($\varepsilon_f^*=0.006$) [2]. The values of σ_o (1198 MPa) and E (147.5 GPa) used to model K_{IH} [2, 11] are used in this study. In addition, the characteristic distance, l^*, is assumed to equal the average carbide spacing (35 μm), since this feature governed hydrogen-induced slip-band fracture for both hydrogen-charged fracture toughness tests and slow crack growth tests at low gas pressures [2, 11].

Model predictions of K_{TH}, assuming strain-controlled slip-band fracture at all grain sizes, are shown in Figure 2. Predicted values of K_{TH} are constant since ε_f^* was assumed to be independent of grain size. This trend parallels that measured for K_{IH} [2, 6], but predicted K_{TH} values are lower because of the elevated crack-tip hydrogen concentration.

TABLE 2
LOCAL FRACTURE STRAIN FOR IN903 AS A FUNCTION OF HYDROGEN CONCENTRATION

Hydrogen Concentration (appm)	Fracture Strain, ε_f^*
0	0.045
770	0.033
1876	0.030
2900	0.021
5000	0.016
$11{,}200^{+}$	0.006^{++}

$^{+}$Estimated for crack tip exposed to 207 MPa H_2 gas
$^{++}$Extrapolated from values at 0 to 5000 appm hydrogen

Comparing predictions from the strain-controlled slip-band cracking model to those based on the stress-controlled intergranular fracture model in Figure 2 indicate that a fracture-mode transition is possible. Predicted K_{TH} values are lower for the stress-based model at grain sizes up to about 100 μm. Above a grain size of 100 μm, predicted K_{TH} values are lower for the strain-based model. These model results suggest that the resistance to stress-based intergranular cracking is lower than the resistance to strain-based slip-band fracture at small grain sizes. The trend is inverted at larger grain sizes; i.e., the resistance to slip-band fracture is lower than the resistance to intergranular cracking. The fracture-mode trend predicted from K_{TH} modeling in Figure 2 is consistent with observations of near-threshold slow crack growth, as slip-band cracking predominated over intergranular fracture at large grain sizes (Figure 1(d)). In addition, measured K_{TH} values follow the lower-bound model predictions (Figure 2), *viz*, K_{TH} increases as grain size increases from 23 μm then appears to reach a plateau value at larger grain sizes.

Analysis of near-threshold slow crack growth results using micromechanical models shows that fracture-mode transitions in IN903 exposed to hydrogen gas can be attributed to competing hydrogen-induced fracture mechanisms. The transition from intergranular cracking to slip-band fracture (Figure 1(b) compared to Figure 1(d)) resulted from the governing effect of the characteristic microstructural distance for intergranular fracture. As the characteristic microstructural distance (grain size) in the stress-based model increased, higher K levels were predicted for intergranular cracking. This increase in intergranular cracking resistance allowed slip-band fracture to proceed preferentially.

The idea that the characteristic microstructural distance for intergranular fracture governs the grain size-dependent fracture mode in stage I can be applied to understand the K-dependent fracture transition in large-grain-size IN903. Specifically, the fracture mode transitions from intergranular cracking in stage II (Figure 1(c)) to slip-band failure in stage I (Figure 1(d)). Assuming that grain size defines the salient distance for intergranular cracking, this transition can be explained because changes in K affect the volume of material at the crack tip that is enveloped by high stress and strain. At low K levels near threshold, the distance over which high stress and strain are sustained may be less than the fracture distance (grain size), which allows slip-band fracture to preempt intergranular cracking. As K increases, high stress and strain are sustained over larger distances that may be comparable to the grain size; intergranular fracture can then be activated.

The idea that fracture-mode transitions in large-grain-size IN903 are due to the interplay between K-dependent crack-tip stress and strain fields and an invariant characteristic distance for intergranular fracture is not supported by analysis of stage II crack growth kinetics. A recent review of hydrogen-induced crack growth rate data in stage II suggests that hydrogen penetration ahead of the crack tip and the associated fracture distances are well less than 1 μm [12]. Included in this analysis are stage II slow crack growth results for IN903 in high-pressure hydrogen gas. This analysis contradicts the assumption that fracture distances on the order of the grain size can account for K-dependent fracture-mode transitions in large-grain-size IN903. Reconciling the contradictory views that near-threshold fracture can be characterized by micrometer-sized, microstructure-relevant fracture distances, while stage II crack growth kinetics require sub-micrometer fracture distances, is a topic that will be addressed in future work.

CONCLUSIONS

The near-threshold fracture mode of IN903 exposed to hydrogen gas exhibits a transition from intergranular cracking to slip-band failure as grain size increases, which results from competing hydrogen-induced fracture mechanisms. A stress-based micromechanical fracture model predicts that the resistance to intergranular cracking increases with increasing grain size. In addition, a strain-based model predicts that the grain size-independent slip-band fracture resistance is of the same order as the intergranular cracking resistance. The predicted fracture-resistance trends intersect at a grain size of about 100 μm, which supports the observed fracture-mode transition between grain sizes of 49 μm and 114 μm.

ACKNOWLEDGEMENTS

The authors are grateful to R.P. Gangloff for critically reviewing the manuscript. This work was supported by the U.S. Department of Energy under contract DE-AC04-94AL85000.

REFERENCES

1. Moody, N.R., Stoltz, R.E. and Perra, M.W. (1986). In: *Corrosion Cracking*, pp. 43-53, Goel, V.S. (Ed). ASM, Metals Park, OH.
2. Moody, N.R., Robinson, S.L. and Garrison, W.M. (1990) *Res Mechanica* 30, 143.
3. Harris, T.M. and Latanision, R.M. (1990). In: *Hydrogen Effects on Material Behavior*, pp. 133-142, Moody, N.R. and Thompson, A.W. (Eds). TMS,Warrendale, PA.
4. Tsuru, T. and Latanision, R.M. (1982) *Scripta Metall.* 16, 575.
5. Moody, N.R., Perra, M.W. and Robinson, S.L. (1988) *Scripta Metall.* 22, 1261.
6. Moody, N.R., Stoltz, R.E. and Perra, M.W. (1987) *Metall. Trans. A* 18A, 1469.
7. Tracey, D.M. (1976) *J. Eng. Mat. Tech. Trans. ASME* 98, 146.
8. Schwalbe, K.-H. (1977) *J. Eng. Mat. Tech. Trans. ASME* 99, 186.
9. Ritchie, R.O. and Thompson, A.W. (1985) *Metall. Trans. A* 16A, 233.
10. Lee, S., Majno, L. and Asaro, R.J. (1985) *Metall. Trans. A*, 16A, 1633.
11. Moody, N.R., Perra, M.W. and Robinson, S.L. (1990). In: *Hydrogen Effects on Material Behavior*, pp. 625-635, Moody, N.R. and Thompson, A.W. (Eds). TMS, Warrendale, PA.
12. Gangloff, R.P. (2001) "Diffusion Control of Hydrogen Environment Embrittlement in High Strength Alloys," submitted to *International Conference on Hydrogen Effects on Material Behavior and Corrosion Deformation Interactions*.

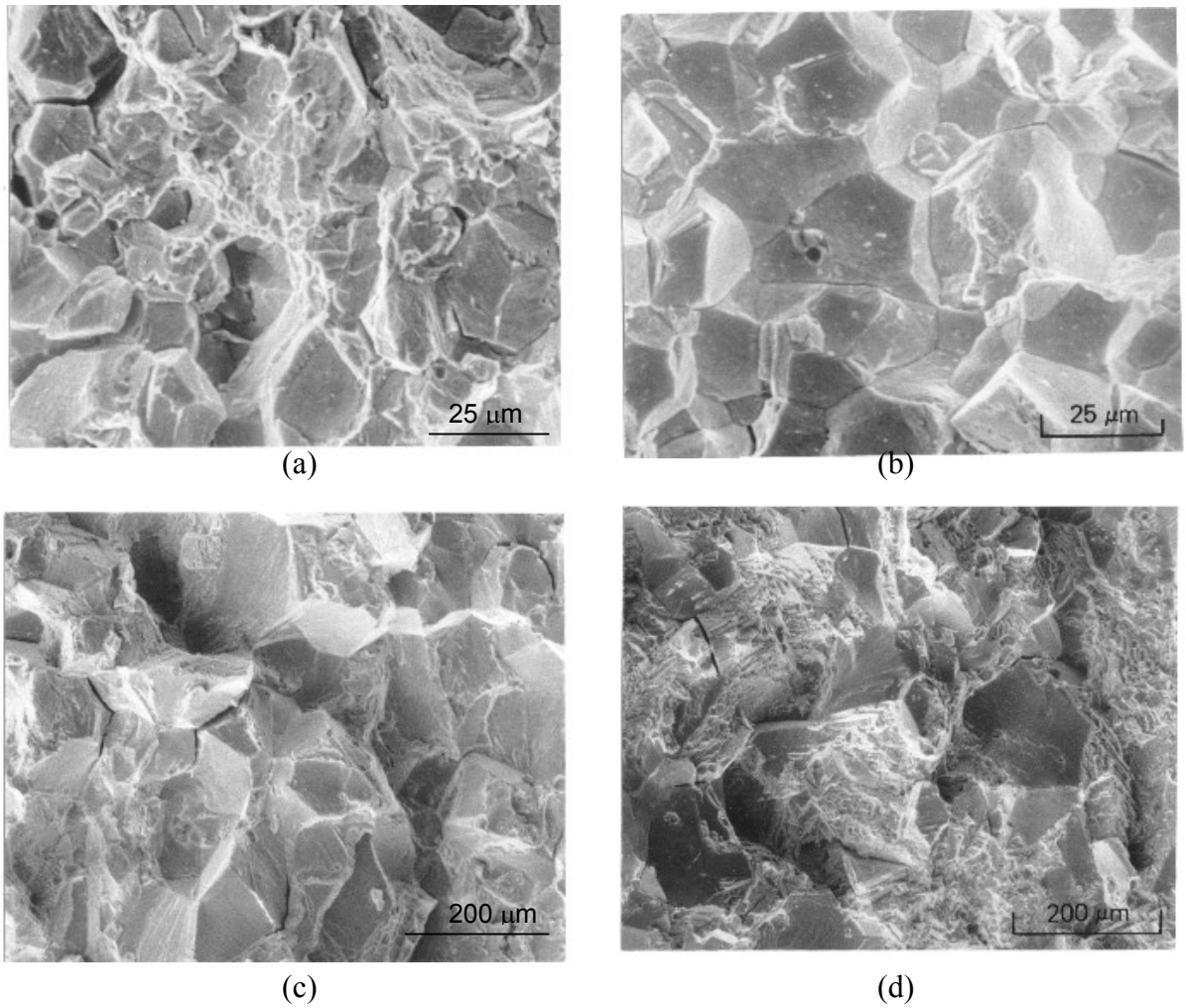

Figure 1: Fracture surfaces for IN903 in 207 MPa hydrogen gas at 25°C: (a) intergranular cracking for 23 μm grain size at K=70 MPa√m, (b) intergranular cracking for 23 μm grain size at K=30 MPa√m, (c) intergranular cracking for 172 μm grain size at K=70 MPa√m, and (d) slip-band and intergranular cracking for 172 μm grain size at K=41 MPa√m.

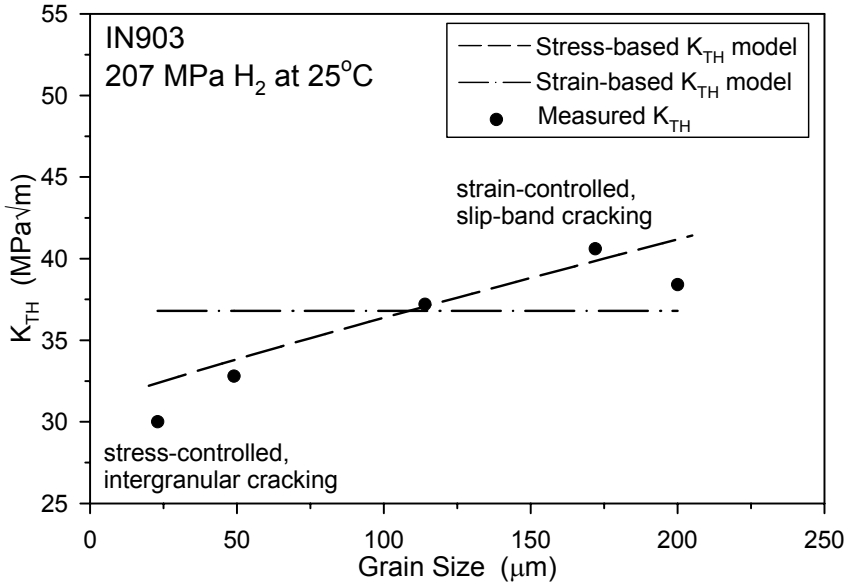

Figure 2: Comparison of K_{TH} from stress-based and strain-based micromechanical fracture models to measured values of K_{TH} for IN903 in 207 MPa hydrogen gas at 25°C.